



# The Role of Cerebrovascular-Reactivity Mapping in Functional MRI: Calibrated fMRI and Resting-State fMRI

J. Jean Chen<sup>1,2\*</sup> and Claudine J. Gauthier<sup>3,4</sup>

<sup>1</sup> Baycrest Centre for Geriatric Care, Rotman Research Institute, Toronto, ON, Canada, <sup>2</sup> Department of Medical Biophysics, University of Toronto, Toronto, ON, Canada, <sup>3</sup> Department of Physics, Concordia University, Montreal, QC, Canada, <sup>4</sup> Montreal Heart Institute, Montreal, QC, Canada

## OPEN ACCESS

### Edited by:

Molly G. Bright,  
Northwestern University,  
United States

### Reviewed by:

Joana Pinto,  
University of Oxford, United Kingdom  
Peiyang Liu,  
Johns Hopkins Medicine,  
United States

### \*Correspondence:

J. Jean Chen  
jchen@research.baycrest.org

### Specialty section:

This article was submitted to  
Vascular Physiology,  
a section of the journal  
Frontiers in Physiology

**Received:** 22 January 2021

**Accepted:** 02 March 2021

**Published:** 25 March 2021

### Citation:

Chen JJ and Gauthier CJ (2021)  
The Role  
of Cerebrovascular-Reactivity  
Mapping in Functional MRI:  
Calibrated fMRI and Resting-State  
fMRI. *Front. Physiol.* 12:657362.  
doi: 10.3389/fphys.2021.657362

Task and resting-state functional MRI (fMRI) is primarily based on the same blood-oxygenation level-dependent (BOLD) phenomenon that MRI-based cerebrovascular reactivity (CVR) mapping has most commonly relied upon. This technique is finding an ever-increasing role in neuroscience and clinical research as well as treatment planning. The estimation of CVR has unique applications in and associations with fMRI. In particular, CVR estimation is part of a family of techniques called calibrated BOLD fMRI, the purpose of which is to allow the mapping of cerebral oxidative metabolism (CMRO<sub>2</sub>) using a combination of BOLD and cerebral-blood flow (CBF) measurements. Moreover, CVR has recently been shown to be a major source of vascular bias in computing resting-state functional connectivity, in much the same way that it is used to neutralize the vascular contribution in calibrated fMRI. Furthermore, due to the obvious challenges in estimating CVR using gas challenges, a rapidly growing field of study is the estimation of CVR without any form of challenge, including the use of resting-state fMRI for that purpose. This review addresses all of these aspects in which CVR interacts with fMRI and the role of CVR in calibrated fMRI, provides an overview of the physiological biases and assumptions underlying hypercapnia-based CVR and calibrated fMRI, and provides a view into the future of non-invasive CVR measurement.

**Keywords:** calibrated BOLD, neurovascular coupling, cerebrovascular reactivity, resting-state fMRI, functional connectivity

## BOLD SIGNAL PHYSIOLOGY

Functional MRI (fMRI) is predominantly performed using the blood-oxygenation level-dependent (BOLD) signal. This signal is based on the paramagnetic properties of deoxyhemoglobin, providing a sensitive, but un-specific marker of neuronal activity. This lack of specificity stems from the fact that most deoxyhemoglobin (dHb) locally arises from baseline metabolism, with a more modest contribution from task-evoked neuronal activity. The signal measured during a task is due to the dilution of these two sources of dHb from a feedforward cascade of events leading to vasodilation in arterioles, bringing fully oxygenated, and therefore diamagnetic, blood to the area of activity (Girouard and Iadecola, 2006; Iadecola, 2017). Therefore, rather than being a direct marker of neuronal activity, the BOLD signal reflects the relative interplay between baseline oxidative

metabolism, task-evoked metabolism, neurovascular coupling mechanisms, and the extent to which local vessels dilate in response to these neurovascular coupling chemical signals (Gauthier and Fan, 2019). It is this last aspect that underlies the amplitude of the cerebrovascular reactivity (CVR) response measured by BOLD fMRI.

While BOLD-based fMRI is widely used and has several applications in clinical fields (Chen, 2018, 2019; Gauthier and Fan, 2019; Specht, 2019), its physiologically unspecific nature makes it vulnerable to a variety of biases, especially in clinical populations (Ances et al., 2011; De Vis et al., 2015; Lajoie et al., 2017; Mazerolle et al., 2018; Chen, 2019). These biases can be vascular in nature, such as differences in baseline blood flow or reactivity, which are known to be prevalent in aging and clinical populations, or maybe due to decline in the availability of neuronal resources. It has been estimated that in healthy brains, the vascular response component is about twice the amplitude of the metabolic response (Hoge et al., 1999a; Uludağ et al., 2004). The vascular response consists of both a blood flow and a blood volume response, but because blood flow has a supralinear dependence on vessel diameter (modeled using Poiseuille's law), it is the blood flow response that dominates the BOLD response. In less healthy populations, changes in vascular elasticity or neurovascular coupling mechanisms can lead to reduced vasodilation (Girouard and Iadecola, 2006; Iadecola, 2017). Because of this supralinear dependence on diameter, even small differences in diameter changes with aging or disease can have a large impact on blood flow as compared to young healthy populations. Therefore, the different physiological sub-components that make up the BOLD signal may not contribute identically to the measured signal in populations of different ages or presenting with different health conditions. This can lead to systematic biases in many BOLD signal comparisons across groups (Gauthier et al., 2012).

## BOLD Sensitivity to CO<sub>2</sub>

In the past decades, the CO<sub>2</sub>-driven BOLD response has been the preeminent method for mapping CVR. CO<sub>2</sub> is a potent vasodilator used that has been shown to rely mainly on the nitric oxide (NO) pathway to increase arterial diameter (Pelligrino et al., 1999; Najarian et al., 2000; Peebles et al., 2008; Iadecola, 2017). While the exact source of NO (endothelial, neuronal or astrocytic) is still debated, NO production has been shown to mirror changes in CO<sub>2</sub> partial pressure, with for example a 40% increase in CO<sub>2</sub> partial pressure resulting in a 36% increase in NO production through endothelial cells in Fathi et al. (2011). Vessel diameter is highly sensitive to the surrounding CO<sub>2</sub> concentration, with increasing CO<sub>2</sub> partial pressures leading to linear increases in both vessel diameter and flow (Hülsmann and Dubelaar, 1988; Komori et al., 2007). In Komori et al. (2007) for example, this increase was shown to be of 21.6% for arteriolar diameter and 34.5% flow velocity for a 50% change in CO<sub>2</sub> partial pressure in rabbit arterioles. This sensitivity can be captured using MRI, within our own data, a 12.0% change in inhaled CO<sub>2</sub> concentration resulting in a 24.9% change in gray matter CBF measured using arterial spin labeling (ASL) and a 1.5% change in the gray matter BOLD signal (Gauthier and Hoge, 2013).

Since the BOLD signal has both a static and temporal signal-to-noise ratio (SNR) that is typically above 100 (Triantafyllou et al., 2005; Gauthier and Hoge, 2013), it is a sensitive measure of CO<sub>2</sub>-induced vasodilation at the whole-brain level.

To induce a BOLD response to CO<sub>2</sub>, either hypercapnia and hypocapnia could be used. Hypercapnia is easier to achieve with more robust BOLD responses, while hypocapnia can be achieved with prospective targeting (Halani et al., 2015), hyperventilation (Cohen et al., 2002), or cued deep breathing (Bright et al., 2009). The various methods for producing CO<sub>2</sub> variations are summarized in a number of recent reviews (Fierstra et al., 2013; Chen, 2018; Pinto et al., 2020).

## THE ROLE OF CVR IN CALIBRATED fMRI

There exists a variety of methods to extract or correct the BOLD signal and make it a more quantitative marker of neuronal activity (Hoge, 2012; Gauthier and Fan, 2019). Notably, CVR is a key component of a family of techniques called calibrated fMRI, which is the predominant approach to quantify and extract the neuronal and vascular components of the BOLD response (Davis et al., 1998; Hoge et al., 1999a,b; Chiarelli et al., 2007; Gauthier and Hoge, 2012). In its fuller implementations, calibrated fMRI allows the separation of the BOLD signal into its baseline and task-induced vascular and metabolic components (Bulte et al., 2012; Gauthier and Hoge, 2012; Wise et al., 2013). In this review, the role of CVR in calibrated fMRI will be discussed.

### What Is Calibrated fMRI?

In its most common form, calibrated fMRI uses breathing manipulations to estimate the blood flow and blood volume component of the BOLD response to a task, in order to separate it from the non-vascular component of the BOLD signal (Davis et al., 1998; Hoge et al., 1999a,b; Chiarelli et al., 2007; Gauthier and Hoge, 2012). The most common calibration procedure for this type of technique uses hypercapnia or increased CO<sub>2</sub> concentration in inhaled air, to cause a putatively purely vascular response (Davis et al., 1998; Hoge et al., 1999a). This calibration procedure is based on the underlying assumption that CO<sub>2</sub>, known to be a potent vasodilator, does not cause any change in oxidative metabolism. This vascular CO<sub>2</sub> response is essentially CVR.

$$M = \frac{\Delta \text{BOLD}/\text{BOLD}_0}{1 - (\text{CBF}/\text{CBF}_0)^{\alpha-\beta}} \quad (1)$$

The original calibrated fMRI model was presented by Davis et al. (1998), followed in 1999 by a more complete description of the dHb dilution model that underlies it by Hoge et al. (1999a). In this model, the BOLD signal measured during hypercapnia is related to the CBF signal measured using ASL during hypercapnia, the calibration M parameter, and two other parameters typically assumed from the literature:  $\alpha$ , which represents flow-volume coupling, and  $\beta$ , which represents the field strength-dependent magnetic properties of dHb. The M parameter is given by Eq. 1. The BOLD and CBF components can be measured, while alpha and beta are assumed, and M is the output of this calibration procedure. Conceptually, M represents the maximum possible

BOLD signal. Since hypercapnia is assumed to be metabolically neutral, then  $M$  corresponds to the BOLD signal one would obtain if all dHb present in the brain from baseline metabolism were suddenly removed. At 3T, this value has been found to be between 4 and 12% when using a hypercapnia model see review in Hoge (2012), Blockley et al. (2015), Mark et al. (2015), and Gauthier and Fan (2019). To perform a calibrated fMRI experiment, therefore, one measures the BOLD and CBF percent signal change in response to mild hypercapnia, then uses the calibration equation from the model to extrapolate to the asymptote of the curve, corresponding to this maximal dilution of dHb. CVR is an intermediate measurement of this technique since it is measured as the BOLD or CBF percent change per mmHg change in  $\text{CO}_2$  concentration during hypercapnia.

The next step of the calibrated fMRI framework per the Davis model is then to estimate the oxidative metabolism component of the BOLD signal measured in response to a task, by combining the  $M$  parameter already measured, the BOLD signal measured in response to the task, the CBF signal measured in response to the same task, and the same alpha and beta parameters mentioned in the calibration procedure. These alpha values are assumed to be the same for the task and calibration (essentially CVR) procedures in most cases, though some work has shown that these may in fact be different (Chen and Pike, 2009, 2010b). It is also noteworthy that some work has suggested that the model should be treated as a heuristic model, rather than a biophysical model and that the value of alpha and beta can in fact be determined through data fitting, resulting in a different set of values than what has typically been used in the literature (Griffeth and Buxton, 2011).

Other versions of calibrated fMRI have been developed following this initial formulation. The simplest version consists in normalizing the BOLD signal from a task by the measured CVR (Bandettini and Wong, 1997; Biswal et al., 2007; Liu et al., 2013). These other models are based on other breathing manipulations such as hyperoxia (Chiarelli et al., 2007) or a combination of hypercapnia and hyperoxia (Gauthier and Hoge, 2012). While hyperoxia-based calibration improves comfort and has been shown to lead to reliable estimates of  $M$  and  $\text{CMRO}_2$ , there is evidence that this model underestimates the true  $M$  and  $\text{CMRO}_2$  (Gauthier and Hoge, 2012). Furthermore, this implementation does not allow estimation of CVR as an intermediate byproduct, which may be valuable in several clinical populations. Finally, extensions of these calibrated fMRI models have also been developed to measure metabolism at rest (Bulte et al., 2012; Gauthier and Hoge, 2012; Wise et al., 2013). These other techniques have been reviewed elsewhere (Gauthier and Fan, 2019).

## The Role of CVR in Calibrated fMRI

The most common calibrated fMRI technique is based on the important assumption that  $\text{CO}_2$  inhalation is metabolically neutral. At high doses,  $\text{CO}_2$  is likely to cause changes in metabolism, but it is typically assumed that the smaller concentrations used in calibrated fMRI (on the order of 5%  $\text{CO}_2$  in most cases) cause negligible changes in metabolism. This is a debated assumption, however, with some studies showing

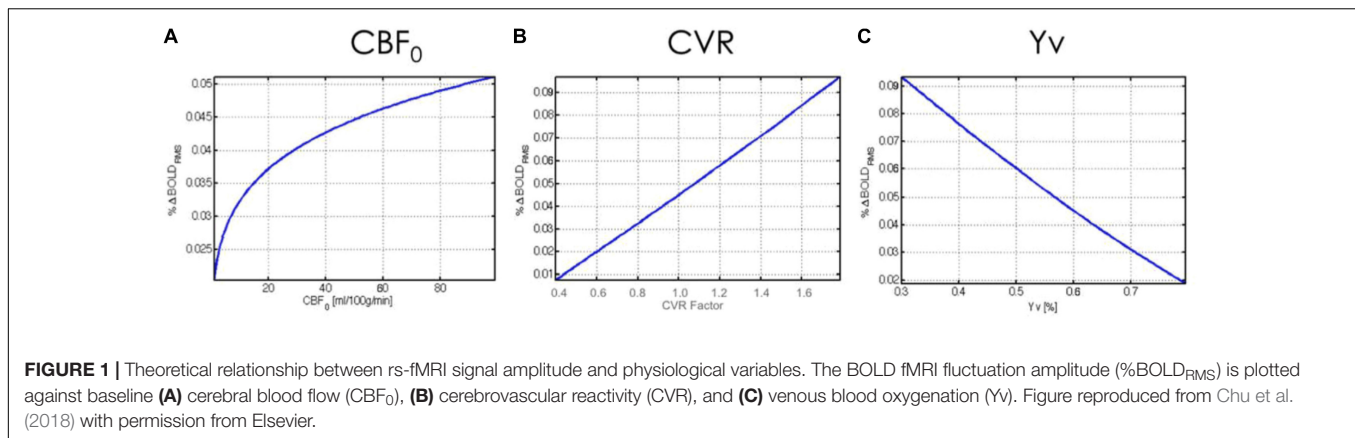
decreased metabolism during  $\text{CO}_2$  inhalation (Xu et al., 2011; Driver et al., 2017) and some showing no change (Chen and Pike, 2010a; Jain et al., 2011). Aside from the difficulty in proving the null hypothesis that  $\text{CO}_2$  is metabolically neutral, whether metabolic activity is detected in response to  $\text{CO}_2$  may be dependent on the technique and the hypercapnia level used to measure it. If hypercapnia does impact oxidative metabolism, and thus biases the CVR estimate used in the calibration step, an accurate measurement of this bias is crucial, as it has been shown to have a large impact on the output of the calibrated fMRI model (Blockley et al., 2015). However, correction of the model to account for the change in  $\text{CMRO}_2$  would be straightforward should an accurate measurement of this effect arise as a  $\text{CMRO}_2$  change parameter could be added to the  $M$  equation rather than assuming a value of one (Blockley et al., 2015; Driver et al., 2017).

Another important consideration is the presence of non-linearities and spatial heterogeneities in the BOLD and underlying CBF response to hypercapnia. It has been shown that the dose-response curve for the CBF and BOLD responses to graded hypercapnia follows a sigmoidal shape, with lower CBF and BOLD responses in the hypocapnic range, as well as saturation effects in the very high inhaled  $\text{CO}_2$  concentration range (Tancredi et al., 2012; Duffin et al., 2017). Therefore, correction by CVR or calibrated fMRI must be interpreted with caution when operating outside the more linear range around 35–50 mmHg (Tancredi et al., 2012). Furthermore, the BOLD, and perhaps even more so, the CBF response to hypercapnia has been shown to be spatially heterogeneous (Gauthier et al., 2012; Tancredi et al., 2012; De Vis et al., 2015). Because of this, it is crucial that regional or voxel-wise measurements of CVR or  $M$  be used to validly inform the BOLD signal or performing calibrated fMRI.

## Assumptions in Calibrated fMRI

The Davis model also assumes that arterial blood is fully oxygenated. This is generally a reasonable assumption, as normal oxygen saturation for arterial blood is typically in the range of 97–100% in young subjects (Barratt-Boyes and Wood, 1957). However, this assumption may be problematic in older (Hardie et al., 2004) and diseased populations (Cukic, 2014; Slowik and Collen, 2020), which could suffer from lower saturations. However, modeling of the effects of anemia has shown that anemia has a very limited impact on the results of the model (Blockley et al., 2015).

Another underlying assumption of this technique is that the chemical signaling that underlies the neurovascular response is comparable to the signaling that underlies  $\text{CO}_2$ -mediated vasodilation. This is because unless these two types of signaling are comparable, then using hypercapnia to assess the vascular response corresponding to a functional task may be misleading and be associated with the very systematic biases between populations that calibrated fMRI was designed to address. Neurovascular coupling is a complex orchestration of signals with many cell types and pathways involved. Detailed studies have shown that when they are active, neurons and interneurons release NO, and that this leads to vasodilation at the arteriolar level (Faraci and Brian, 1994; Rancillac et al., 2006;



Attwell et al., 2010; Iadecola, 2017). Capillary dilation is, however, dependent on astrocytic activation of other pathways, especially the arachidonic acid pathway (Mishra et al., 2016). Nevertheless, it has been shown that inhibition of nNOS leads to an almost complete diminution of the BOLD and CBF response to neuronal stimulation in rat (Stefanovic et al., 2007), establishing nNOS as one of the main mediators of the neurovascular coupling that underlies the fMRI signals.

The vasodilatory response to hypercapnia on the other hand has been shown to be predominantly due to activation of the NOS pathway, leading to the release of NO from neurons (Pelligrino et al., 1999) and endothelial cells (Najarian et al., 2000; Peebles et al., 2008). When the NO pathway is blocked, the vasodilatory response is reduced by 36–94% depending on the inhibitor used, hypercapnia levels and species (Iadecola and Zhang, 1994). While some studies have shown that inhibiting the endothelial NO pathway or destroying endothelial cells does not abolish the CBF response to hypercapnia (Wang et al., 1994), other studies have shown that neuronal sources cannot in isolation explain the CBF response to hypercapnia (Iadecola et al., 1987, 1993; Iadecola and Zhang, 1996). This likely reflects a combined contribution of endothelial and neuronal sources or redundancy that allows one system to come online when the other fails. It is important to note, however, that there may be some important species-related differences in pathways (Najarian et al., 2000), making animal results only partly relevant to human data. Therefore, while it is currently unclear whether these two responses are truly equivalent, there are clear similarities between them, lending validity to the use of hypercapnia-based CVR as a model for the vascular component of neurovascular coupling.

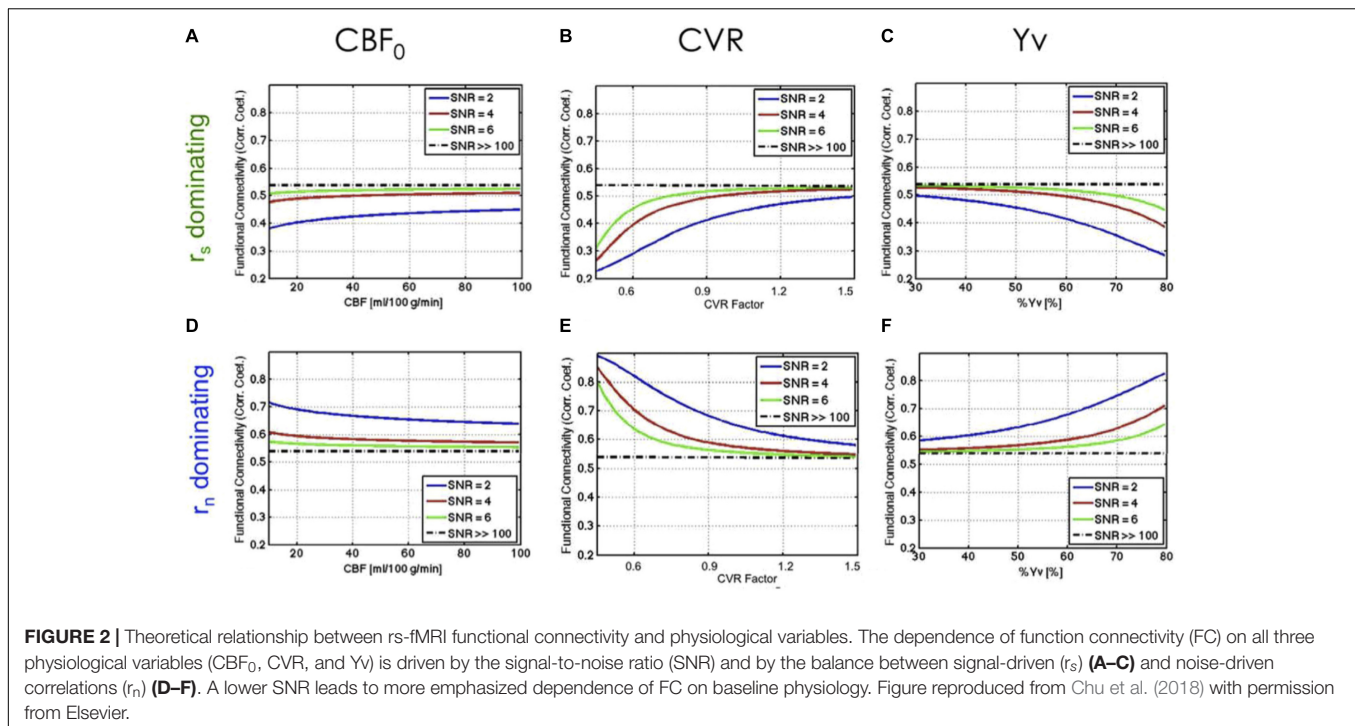
## THE ROLE OF CVR IN RESTING-STATE fMRI

### What Is Resting-State fMRI?

Functional MRI in the resting state (rs-fMRI), particularly based on the BOLD signal, has been extensively used to measure functional connectivity in the brain. The use of the BOLD signal for resting-state imaging largely began with the seminal discovery of resting-state BOLD signal-based (rs-BOLD)

synchronization across brain networks (namely “resting-state functional connectivity”) by Biswal et al. (Biswal et al., 1995; Fox, 2010). Despite the undefined cognitive state of the brain in the “resting-state” and the ambiguous involvement of vascular and metabolic mechanisms underlying the BOLD signal (discussed later in this section), resting-state BOLD signal-based brain networks have been consistently revealed in numerous studies. Notably, the well-documented default-mode network (DMN), key in generating cognition, has been implicated in a wide array of neurological diseases. In recent years, resting-state BOLD-fMRI has gained considerable attention in basic and clinical neuroscience (Biswal et al., 1995; Fox, 2010) and the number of publications using the resting-state BOLD contrast has seen exponential growth. This remarkable growth is attributable to the ability of rs-BOLD studies to bypass the hurdles of task performance and behavioral evaluations in assessing brain function, opening a new attractive avenue for neuroimaging research in pediatrics, aging, and a variety of neurologic and psychiatric diseases. A comprehensive description of the applications of rs-BOLD signals can be found in recent reviews (Fox, 2010).

Functional connectivity is the main reason for the popularity of resting-state fMRI. First-level resting-state functional connectivity is generally computed using seed-based correlation or data-driven approaches. In the model-based seed-correlation analysis (Biswal et al., 1995; Van Dijk et al., 2010), connectivity is defined as the correlation between the seed rs-fMRI signal time series and those of other brain voxels or regions. Data-driven methods typically use principal- or independent component analysis (PCA and ICA, respectively) to identify brain networks. While the seed-based approach is constrained by model assumptions and *a priori* hypotheses, model-free data-driven methods are more challenging to use in group-analyses due to higher variability in the network components identified. Seed- and data-driven approaches yield largely similar spatial patterns (although with differing spatial extents), and both methods can be used to determine connectivity magnitude. However, due to the linear assumptions related to the model-based connectivity methods, it is easier to intuit the influence of physiological metrics on resting-state functional connectivity. After all, there is a well-defined relationship between the correlation coefficient



and the rs-fMRI signal amplitude, which is, in turn, describable by the steady-state fMRI signal model as introduced earlier. With the adoption of higher-level functional connectivity measures (those derived from the first-level metrics, such as centrality and hubness, to name a few), the effect of physiological biases may not seem obvious, but it is all the more important to understand them at more abstract levels of analysis.

### The Role of CVR in Resting-State fMRI

The rs-fMRI technique, while immensely popular, has been limited by a lack of a fundamental physiological understanding of the underlying rs-fMRI BOLD signal (Leopold and Maier, 2012). The BOLD signal is only an indirect measure of neuronal activity and is inherently modulated by both neuronal activity and vascular physiology (Biswal et al., 2007; Kannurpatti et al., 2008; Biswal and Kannurpatti, 2009; Tong and Frederick, 2010). Currently, the respective contributions of these factors to resting-state BOLD are still unknown. This knowledge gap leads to great challenges for data interpretation in clinical scenarios, whereby these contributions are often altered. The literature suggests that BOLD-based fMRI signal is fundamentally modulated by local vascular physiology (Carusone et al., 2002; Kannurpatti et al., 2010; Liu, 2013).

Previous work on the biophysical origins of the rs-fMRI signal suggests that the steady-state BOLD model (Davis et al., 1998; Hoge et al., 1999a), as outlined in the previous section, is a reasonable framework for understanding the neurovascular underpinnings of the resting BOLD effect. CVR is known to covary with the BOLD response to neuronal activation (Stefanovic et al., 2006). Specifically, reduced vascular responsiveness has been associated with reduced BOLD activation amplitude as well as a slowing down in the BOLD response dynamics (Behzadi and Liu, 2005; Rack-Gomer and Liu,

2012), setting the stage for our study of the effect of CVR on the rs-fMRI signal. Indeed, CVR is a major factor determining the hemodynamic response to neuronal activity, which in turn modulates rs-fMRI signal amplitude [see review (Liu, 2013) and Figure 1]. As a result, CVR is expected to drive the amplitude of resting BOLD signal fluctuations (RSFA). Indeed, hypercapnia, which elevates basal CBF and oxygenation while reducing CVR (Cohen et al., 2002), has been shown to reduce the amplitude of resting-state BOLD signals (Biswal et al., 1997; Xu et al., 2011), consistent with predictions based on the BOLD signal model. Although hypercapnia has also been shown to reduce the power of the alpha-rhythm (Xu et al., 2011), CVR is likely to also play a key role in modulating the RSFA in this context. As an extension, in a study of 335 healthy older adults (Tsvetanov et al., 2015), it was found that the effects of aging on the RSFA were mediated by cardiovascular factors such as heart rate.

Interestingly, another representation of the rs-fMRI signal fluctuation, the amplitude of low-frequency fluctuations (ALFF), is typically interpreted as a neuronal measure (Zou et al., 2008; Jia et al., 2020). It is important to realize that the RSFA and ALFF are directly proportional to each other and that it is illogical to interpret the same quantity in two different ways. Furthermore, the fractional ALFF (fALFF) amounts to the RSFA normalized by the per-voxel signal variance instead of the mean (Zou et al., 2008; Jia et al., 2020). This measure would be influenced by both the neuronal signal content at the SNR at each voxel, making the physiological interpretation more tortuous.

However, the relationship between the RSFA and functional connectivity is more subtle than linear. The hemodynamic response determines the BOLD signal amplitude and subsequently the rs-fMRI BOLD SNR; different signal SNRs will in turn lead to different connectivity measurements (Liu, 2013). Such biases may obscure the meaning of rs-fMRI functional

connectivity measurements (Golestani et al., 2016; Chu et al., 2018), which are modulated by the RSFA (Rack-Gomer and Liu, 2012; Tak et al., 2015).

In our previous work (Golestani et al., 2016), we demonstrated the extent of this modulation, as well as uncovered the effect of CVR modulation on rs-fMRI functional connectivity. Across the group, rs-fMRI functional connectivity of the motor network also depends significantly on the baseline capnic state, with the hypocapnic baseline associated with the highest connectivity values, and hypercapnic baseline associated with the lowest connectivity. The latter finding is in agreement with early data from Biswal et al. (1997) and from more recent data from Xu et al. (2011). This association, however, is not consistent across the brain. The recent work by Lewis et al. (2020) extends this work to dynamic functional-connectivity analyses and over 42 functional networks. It was found that network connectivity is generally weaker during vasodilation, which is supported by previous research (Biswal et al., 1997; Golestani et al., 2016).

As follow-up work (Chu et al., 2018), instead of modulating CVR within individuals, we compared fcMRI and CVR across different individuals. There was observable inter-subject CVR variation even amongst healthy young adults, as well as a distribution of functional connectivity values. In this work, we used the steady-state BOLD model to make predictions about functional connectivity given CVR (as well as CBF and  $SO_2$ ) (Figure 2). We further used these predictions to help interpret the empirical data, with the objective of improving our understanding of the possible origins of inter-subject variations in rs-fMRI functional connectivity. However, the characterization of vascular biases on rs-fMRI metrics remains scarce in current literature.

Given the above, the open question is how to normalize or calibrate the vascular effects from rs-fMRI measures, which is especially used to study neuronal markers (Champagne et al., 2020; Coverdale et al., 2020; Tsvetanov et al., 2020). As an example of the application of a normalization approach, Xu et al. (2011) normalized the resting-state BOLD amplitudes in the default-mode network by the task-related BOLD responses in the visual cortex, as  $CO_2$  challenges were observed not to alter the RSFA in the visual cortex. More recently, following the findings in Chu et al. (2018) and Champagne et al. (2020) normalized functional connectivity by local CBF and observed a reduction in connectivity differences between healthy and patient groups. This is in line with observations by Garrett et al. (2017), who also observed age-related differences in RSFA to be reduced when normalized by vascular physiology. However, it is likely that the fcMRI-CVR association is mechanical (driven by local CVR and the local vessel composition) and coincidental (driven by the relationship of both to neuronal health). Hence, adequate correction of vascular bias remains an open challenge.

## Quantifying CVR Using Resting-State fMRI

Resting-state fMRI offers a unique opportunity to glean CVR information without the need for respiratory challenges. This type of “unconstrained” or “task-free” CVR protocol does not

require cooperation from participants, and is thus a promising direction of research that will likely broaden the accessibility of CVR mapping to clinical researchers (Chen, 2018).

The RSFA was initially introduced as a vascular scaling factor for task-based BOLD responses by Kannurpatti et al. (2011), as it was used to scale fMRI task responses in the study of aging. Since then, resting-state methods that do not require  $CO_2$  perturbation have flourished (Golestani et al., 2016; Jahanian et al., 2017; Liu et al., 2017). Notably, Kannurpatti et al. (2014) reported a comparison of the resting-state fMRI fluctuation amplitude (voxel-wise temporal standard deviation) as a CVR surrogate. Liu et al. (2017) introduced a method that uses the low-frequency range of the rs-fMRI signal, regressed against the global-signal, to generate a qualitative CVR estimate. In the same year, Jahanian et al. (2017) introduced the concept of using either the voxel-wise regression coefficients with cerebrospinal fluid signal (measured using rs-fMRI) or using the voxel-wise coefficient of variation to approximate CVR. The former is more akin to the approach of Liu et al. (2017) while the latter follows the logic of the method by Kannurpatti et al. (2014). In the meantime, the Liu method has also been demonstrated in delineating global and local CVR deficits (in Moyamoya disease and acute stroke, respectively) (Taneja et al., 2019).

While all of these methods have demonstrated correlations with  $CO_2$ -based CVR measures, they provide qualitative measures of CVR, which complicates inter-subject comparisons, quantitative CVR mapping techniques using rs-fMRI remain scarce. The only such technique takes advantage of spontaneous fluctuations in end-tidal  $CO_2$  while eliminating the effects of heart-rate and respiratory-volume variability on the fMRI signal (Golestani et al., 2016). Once the  $CO_2$ -related BOLD signal is isolated, a deconvolution is performed between the resting-state fMRI and  $CO_2$  time courses, and the area under the response function is by definition the quantitative CVR. This approach echoes the derivation of the  $CO_2$  response function using a series of breathing maneuvers, including deep breathing, rapid breathing and free breathing (Vogt et al., 2011). The derivation of the whole response function instead of a simple CVR amplitude provides the opportunity to extract temporal CVR features.

As in the case of calibrated fMRI, one should be aware of spatial heterogeneities and non-linearities in the flow and BOLD response to  $CO_2$ . For instance, the use of CVR to normalize rs-fMRI metrics is only a valid approach if one can assume that the CVR response obtained in different individuals and brain regions are taken from the same linear regime.

## Other Vascular Sources of Resting-State fMRI

Beyond the magnitude of CVR, the dynamic features of the fMRI response function that are available through this method can also provide useful information. A slowing of the CVR response has been shown to characterize vascular lesions (Poublanc et al., 2015), adding a dimension to the utility of CVR mapping. Indeed, differences between young and older adults have been demonstrated

using simply the temporal features of the resting CO<sub>2</sub> response function (Esmaelbeigi and Chen, 2019). It is further shown that by accounting for the temporal shifts in the BOLD CO<sub>2</sub> response, improved CVR estimates can be obtained (Yao et al., 2021). Furthermore, this CO<sub>2</sub>-related shift structure can be associated with the lag structure that naturally occurs in the rs-fMRI signal (Tong and Frederick, 2014; Aso et al., 2019), and can be capitalized to extract additional vascular information without CO<sub>2</sub> challenges.

Respiratory-volume variability (RVT) also modulates the rs-fMRI signal (Birn et al., 2006), and a potential relationship between CO<sub>2</sub> and RVT has previously been identified (Vogt et al., 2011). This was extended to the convolution of the RVT with its fMRI response function (Chang and Glover, 2009). Thus, RVT can also be considered as a potential physiological marker to yield a CVR measure, a possible future research direction.

The CO<sub>2</sub> response has also been reported to exhibit network structure that coincide with that of conventional rs-fMRI functional networks (Bright et al., 2020). Cardiac pulsatility, which entrains the autonomic nervous system, is also known to contribute to the rs-fMRI signal in a spatially specific manner (Shmueli et al., 2007; Chang et al., 2009; Shokri-Kojori et al., 2018; Attarpour et al., 2021). In fact, a substantial portion of the rs-fMRI signal may stem from cardiogenic vascular oscillations, and such signals can interact with respiration and CO<sub>2</sub> in a biofeedback loop (Attarpour et al., 2021). Respiratory and cardiac-related physiological networks have recently been documented in detail (Chen et al., 2020).

## CURRENT CHALLENGES AND FUTURE DIRECTIONS

Cerebrovascular reactivity has been found to associate with cerebral autoregulation, which is assessed as the phase shift between arterial blood pressure and venous blood flow changes (Carrera et al., 2009). This association is observed in vascular pathologies (Chen et al., 2014), and can influence the degree to which the vasculature responds to CO<sub>2</sub>. Thus, the use of CVR in calibrated BOLD and resting BOLD can lead to biased results in certain patient populations.

Novel accelerated imaging acquisitions can enhance the power of calibrated and resting-state fMRI. Specifically, the use of multi-echo BOLD in conjunction with simultaneous multi-slice acceleration has led to improved isolation of BOLD from noise contributions in the task and resting fMRI alike (Olafsson et al., 2015) as well as to more robust CVR estimates (Cohen and Wang, 2019). The ability to accelerate acquisitions using slice acceleration has also led to improved efficiency in terms of

sensitivity per unit time for capturing the BOLD response (Todd et al., 2017). Moreover, a slice acceleration factor of up to four can be achieved without sacrificing rs-fMRI data quality (Preibisch et al., 2015), with the time savings opening up possibilities for CVR scans to be included in a typical scan session.

Despite the wide use of calibrated fMRI, the fundamental accuracy of the CO<sub>2</sub>-calibrated BOLD model remains to be validated under different conditions (Hoge, 2012; Blockley et al., 2015; Chen, 2019). While the basic principle of CVR involvement in the BOLD response remains valid, the extent to which different vascular compartments are involved, and the resultant BOLD signal evolution, continue to be refined using electrophysiological recordings (Shmuel et al., 2006; Liu et al., 2010; Sanganahalli et al., 2016), near-infrared spectroscopy (Boas et al., 2003; Gagnon et al., 2012), and two-photon microscopy (Gagnon et al., 2016). In the latter work, the interpretation of the Davis model and the calibration process is revised using microscopy-informed Monte Carlo simulations of the BOLD signal. In rs-fMRI, the desire to isolate the neuronal from the vascular fluctuations has led to the involvement of electroencephalography (EEG) (Chang et al., 2013; Liu et al., 2014) and glucose positron emission tomography (PET) (Thompson et al., 2016). While the approach of normalizing rs-fMRI metrics by CVR may be an oversimplification, it is a viable first step in extracting the neuronal information from fMRI alone.

## CONCLUSION

Cerebrovascular reactivity is important for the interpretation of both task-based and resting-state fMRI results. The need to incorporate CVR into fMRI data interpretation is increasingly recognized, but more accessible ways of mapping CVR are necessary for wide adoption.

## AUTHOR CONTRIBUTIONS

All authors listed have made a substantial, equal, direct and intellectual contribution to the work, and approved it for publication.

## FUNDING

The writing of this review was supported by the Canadian Institutes of Health Research (CIHR), the Heart and Stroke Foundation, and the Michal and Renata Hornstein Chair in Cardiovascular Imaging.

## REFERENCES

- Ances, B., Vaida, F., Ellis, R., and Buxton, R. (2011). Test-retest stability of calibrated BOLD-fMRI in HIV- and HIV+ subjects. *Neuroimage* 54, 2156–2162. doi: 10.1016/j.neuroimage.2010.09.081
- Aso, T., Urayama, S., Fukuyama, H., and Murai, T. (2019). Axial variation of deoxyhemoglobin density as a source of the low-frequency time lag structure in blood oxygenation level-dependent signals. *PLoS One* 14:e0222787. doi: 10.1371/journal.pone.0222787
- Attarpour, A., Ward, J., and Chen, J. J. (2021). Vascular origins of low-frequency oscillations in the cerebrospinal fluid signal in resting-state fMRI: validation using photoplethysmography. *Hum. Brain Mapp.* 1, 1–2. in press.
- Attwell, D., Buchan, A. M., Charpak, S., Lauritzen, M., Macvicar, B. A., and Newman, E. A. (2010). Glial and neuronal control of brain blood flow. *Nature* 468, 232–243. doi: 10.1038/nature09613

- Bandettini, P. A., and Wong, E. C. (1997). A hypercapnia-based normalization method for improved spatial localization of human brain activation with fMRI. *NMR Biomed.* 10, 197–203. doi: 10.1002/(sici)1099-1492(199706/08)10:4/5<197::aid-nbm466>3.0.co;2-s
- Barratt-Boyes, B. G., and Wood, E. H. (1957). The oxygen saturation of blood in the venae cavae, right-heart chambers, and pulmonary vessels of healthy subjects. *J. Lab. Clin. Med.* 50, 93–106.
- Behzadi, Y., and Liu, T. T. (2005). An arteriolar compliance model of the cerebral blood flow response to neural stimulus. *Neuroimage* 25, 1100–1111. doi: 10.1016/j.neuroimage.2004.12.057
- Birn, R. M., Diamond, J. B., Smith, M. A., and Bandettini, P. A. (2006). Separating respiratory-variation-related fluctuations from neuronal-activity-related fluctuations in fMRI. *Neuroimage* 31, 1536–1548. doi: 10.1016/j.neuroimage.2006.02.048
- Biswal, B., Hudetz, A. G., Yetkin, F. Z., Haughton, V. M., and Hyde, J. S. (1997). Hypercapnia reversibly suppresses low-frequency fluctuations in the human motor cortex during rest using echo-planar MRI. *J. Cereb. Blood Flow Metab.* 17, 301–308. doi: 10.1097/00004647-199703000-00007
- Biswal, B., Zerrin Yetkin, F., Haughton, V. M., and Hyde, J. S. (1995). Functional connectivity in the motor cortex of resting human brain using echo-planar mri. *Magn. Reson. Med.* 34, 537–541. doi: 10.1002/mrm.1910340409
- Biswal, B. B., and Kannurpatti, S. S. (2009). Resting-state functional connectivity in animal models: modulations by exsanguination. *Methods Mol. Biol.* 489, 255–274. doi: 10.1007/978-1-59745-543-5\_12
- Biswal, B. B., Kannurpatti, S. S., and Rypma, B. (2007). Hemodynamic scaling of fMRI-BOLD signal: validation of low-frequency spectral amplitude as a scalability factor. *Magn. Reson. Imaging* 25, 1358–1369. doi: 10.1016/j.mri.2007.03.022
- Blockley, N. P., Griffith, V. E. M., Stone, A. J., Hare, H. V., and Bulte, D. P. (2015). Sources of systematic error in calibrated BOLD based mapping of baseline oxygen extraction fraction. *Neuroimage* 122, 105–113. doi: 10.1016/j.neuroimage.2015.07.059
- Boas, D. A., Strangman, G., Culver, J. P., Hoge, R. D., Jaszewski, G., Poldrack, R. A., et al. (2003). Can the cerebral metabolic rate of oxygen be estimated with near-infrared spectroscopy? *Phys. Med. Biol.* 48, 2405–2418. doi: 10.1088/0031-9155/48/15/311
- Bright, M. G., Bulte, D. P., Jezzard, P., and Duyn, J. H. (2009). An alternative technique for measuring cerebrovascular reactivity; comparing cued deep breathing hypocapnia with inspiration of carbon dioxide. *Proc. Intl. Soc. Mag. Reson. Med.* 17, 1634.
- Bright, M. G., Whittaker, J. R., Driver, I. D., and Murphy, K. (2020). Vascular physiology drives functional brain networks. *Neuroimage* 217:116907. doi: 10.1016/j.neuroimage.2020.116907
- Bulte, D. P., Kelly, M., Germuska, M., Xie, J., Chappell, M. A., Okell, T. W., et al. (2012). Quantitative measurement of cerebral physiology using respiratory-calibrated MRI. *Neuroimage* 60, 582–591. doi: 10.1016/j.neuroimage.2011.12.017
- Carrera, E., Lee, L. K., Giannopoulos, S., and Marshall, R. S. (2009). Cerebrovascular reactivity and cerebral autoregulation in normal subjects. *J. Neurol. Sci.* 285, 191–194. doi: 10.1016/j.jns.2009.06.041
- Carusone, L. M., Srinivasan, J., Gitelman, D. R., Mesulam, M.-M., and Parrish, T. B. (2002). Hemodynamic response changes in cerebrovascular disease: implications for functional MR imaging. *AJNR Am. J. Neuroradiol.* 23, 1222–1228.
- Champagne, A. A., Coverdale, N. S., Ross, A., Chen, Y., Murray, C. I., Dubowitz, D., et al. (2020). Multi-modal normalization of resting-state using local physiology reduces changes in functional connectivity patterns observed in mTBI patients. *Neuroimage Clin.* 26:102204. doi: 10.1016/j.nicl.2020.102204
- Chang, C., Cunningham, J. P., and Glover, G. H. (2009). Influence of heart rate on the BOLD signal: the cardiac response function. *Neuroimage* 44, 857–869. doi: 10.1016/j.neuroimage.2008.09.029
- Chang, C., and Glover, G. H. (2009). Relationship between respiration, end-tidal CO<sub>2</sub>, and BOLD signals in resting-state fMRI. *Neuroimage* 47, 1381–1393. doi: 10.1016/j.neuroimage.2009.04.048
- Chang, C., Liu, Z., Chen, M. C., Liu, X., and Duyn, J. H. (2013). EEG correlates of time-varying BOLD functional connectivity. *Neuroimage* 72, 227–236. doi: 10.1016/j.neuroimage.2013.01.049
- Chen, J., Liu, J., Xu, W.-H., Xu, R., Hou, B., Cui, L.-Y., et al. (2014). Impaired dynamic cerebral autoregulation and cerebrovascular reactivity in middle cerebral artery stenosis. *PLoS One* 9:e88232. doi: 10.1371/journal.pone.0088232
- Chen, J. E., Lewis, L. D., Chang, C., Tian, Q., Fultz, N. E., Ohringer, N. A., et al. (2020). Resting-state “physiological networks.”. *Neuroimage* 213:116707. doi: 10.1016/j.neuroimage.2020.116707
- Chen, J. J. (2018). Cerebrovascular-reactivity mapping using MRI: considerations for Alzheimer’s disease. *Front. Aging. Neurosci.* 10:170. doi: 10.3389/fnagi.2018.00170
- Chen, J. J. (2019). Functional MRI of brain physiology in aging and neurodegenerative diseases. *Neuroimage* 187, 209–225. doi: 10.1016/j.neuroimage.2018.05.050
- Chen, J. J., and Pike, G. B. (2009). BOLD-specific cerebral blood volume and blood flow changes during neuronal activation in humans. *NMR Biomed.* 22, 1054–1062. doi: 10.1002/nbm.1411
- Chen, J. J., and Pike, G. B. (2010a). Global cerebral oxidative metabolism during hypercapnia and hypocapnia in humans: implications for BOLD fMRI. *J. Cereb. Blood Flow Metab.* 30, 1094–1099. doi: 10.1038/jcbfm.2010.42
- Chen, J. J., and Pike, G. B. (2010b). MRI measurement of the BOLD-specific flow–volume relationship during hypercapnia and hypocapnia in humans. *Neuroimage* 53, 383–391. doi: 10.1016/j.neuroimage.2010.07.003
- Chiarelli, P. A., Bulte, D. P., Wise, R., Gallichan, D., and Jezzard, P. (2007). A calibration method for quantitative BOLD fMRI based on hyperoxia. *Neuroimage* 37, 808–820. doi: 10.1016/j.neuroimage.2007.05.033
- Chu, P. P. W., Golestani, A. M., Kwint, J. B., Khatamian, Y. B., and Chen, J. J. (2018). Characterizing the modulation of resting-state fMRI metrics by baseline physiology. *Neuroimage* 173, 72–87. doi: 10.1016/j.neuroimage.2018.02.004
- Cohen, A. D., and Wang, Y. (2019). Improving the assessment of breath-holding induced cerebral vascular reactivity using a multiband multi-echo ASL/BOLD sequence. *Sci. Rep.* 9:5079.
- Cohen, E. R., Ugurbil, K., and Kim, S. G. (2002). Effect of basal conditions on the magnitude and dynamics of the blood oxygenation level-dependent fMRI response. *J. Cereb. Blood Flow Metab.* 22, 1042–1053. doi: 10.1097/00004647-200209000-00002
- Coverdale, N. S., Fernandez-Ruiz, J., Champagne, A. A., Mark, C. I., and Cook, D. J. (2020). Co-localized impaired regional cerebrovascular reactivity in chronic concussion is associated with BOLD activation differences during a working memory task. *Brain Imaging Behav.* 14, 2438–2449. doi: 10.1007/s11682-019-00194-5
- Cukic, V. (2014). The changes of arterial blood gases in COPD during four-year period. *Mediev. Archaeol.* 68, 14–18. doi: 10.5455/medarh.2014.68.14-18
- Davis, T. L., Kwong, K. K., Weisskoff, R. M., and Rosen, B. R. (1998). Calibrated functional MRI: mapping the dynamics of oxidative metabolism. *Proc. Natl. Acad. Sci. U. S. A.* 95, 1834–1839. doi: 10.1073/pnas.95.4.1834
- De Vis, J. B., Hendrikse, J., Bhogal, A., Adams, A., Kappelle, L. J., and Petersen, E. T. (2015). Age-related changes in brain hemodynamics; a calibrated MRI study. *Hum. Brain Mapp.* 36, 3973–3987. doi: 10.1002/hbm.22891
- Driver, I. D., Wise, R. G., and Murphy, K. (2017). Graded hypercapnia-calibrated BOLD: beyond the Iso-metabolic hypercapnic assumption. *Front. Neurosci.* 11:276. doi: 10.3389/fnins.2017.00276
- Duffin, J., Sobczyk, O., Crawley, A., Poublanc, J., Venkatraghavan, L., Sam, K., et al. (2017). The role of vascular resistance in BOLD responses to progressive hypercapnia. *Hum. Brain Mapp.* 38, 5590–5602. doi: 10.1002/hbm.23751
- Esmaelbeigi, A., and Chen, J. J. (2019). The effect of age on resting state fMRI carbon dioxide response function. *Proc. Organ. Hum. Brain Mapp.* 2019:1403.
- Faraci, F. M., and Brian, J. E. Jr. (1994). Nitric oxide and the cerebral circulation. *Stroke* 25, 692–703. doi: 10.1161/01.str.25.3.692
- Fathi, A. R., Yang, C., Bakhtian, K. D., Qi, M., Lonser, R. R., and Pluta, R. M. (2011). Carbon dioxide influence on nitric oxide production in endothelial cells and astrocytes: cellular mechanisms. *Brain Res.* 1386, 50–57. doi: 10.1016/j.brainres.2011.02.066
- Fierstra, J., Sobczyk, O., Battisti-Charbonney, A., Mandell, D. M., Poublanc, J., Crawley, A. P., et al. (2013). Measuring cerebrovascular reactivity: what stimulus to use? *J. Physiol.* 591, 5809–5821. doi: 10.1113/jphysiol.2013.259150
- Fox, M. D. (2010). Clinical applications of resting state functional connectivity. *Front. Syst. Neurosci.* 4:19. doi: 10.3389/fnsys.2010.00019
- Gagnon, L., Sakadžić, S., Lesage, F., Pouliot, P., Dale, A. M., Devor, A., et al. (2016). Validation and optimization of hypercapnic-calibrated fMRI from oxygen-sensitive two-photon microscopy. *Philos. Trans. R. Soc. Lond. B Biol. Sci.* 371:20150359. doi: 10.1098/rstb.2015.0359
- Gagnon, L., Yücel, M. A., Dehaes, M., Cooper, R. J., Perdue, K. L., Selb, J., et al. (2012). Quantification of the cortical contribution to the NIRS signal over



- the motor cortex using concurrent NIRS-fMRI measurements. *Neuroimage* 59, 3933–3940. doi: 10.1016/j.neuroimage.2011.10.054
- Garrett, D. D., Lindenberger, U., Hoge, R. D., and Gauthier, C. J. (2017). Age differences in brain signal variability are robust to multiple vascular controls. *Sci. Rep.* 7:10149.
- Gauthier, C. J., and Fan, A. P. (2019). BOLD signal physiology: models and applications. *Neuroimage* 187, 116–127. doi: 10.1016/j.neuroimage.2018.03.018
- Gauthier, C. J., and Hoge, R. D. (2012). Magnetic resonance imaging of resting OEF and CMRO2 using a generalized calibration model for hypercapnia and hyperoxia. *Neuroimage* 60, 1212–1225. doi: 10.1016/j.neuroimage.2011.12.056
- Gauthier, C. J., and Hoge, R. D. (2013). A generalized procedure for calibrated MRI incorporating hyperoxia and hypercapnia. *Hum. Brain Mapp.* 34, 1053–1069. doi: 10.1002/hbm.21495
- Gauthier, C. J., Madjar, C., Desjardins-Crépeau, L., Bellec, P., Bherer, L., and Hoge, R. D. (2012). Age dependence of hemodynamic response characteristics in human functional magnetic resonance imaging. *Neurobiol. Aging* 34, 1469–1485. doi: 10.1016/j.neurobiolaging.2012.11.002
- Girouard, H., and Iadecola, C. (2006). Neurovascular coupling in the normal brain and in hypertension, stroke, and Alzheimer disease. *J. Appl. Physiol.* 100, 328–335. doi: 10.1152/jappphysiol.00966.2005
- Golestani, A. M., Kwinta, J. B., Strother, S. C., Khatamian, Y. B., and Chen, J. J. (2016). The association between cerebrovascular reactivity and resting-state fMRI functional connectivity in healthy adults: the influence of basal carbon dioxide. *Neuroimage* 132, 301–313. doi: 10.1016/j.neuroimage.2016.02.051
- Griffith, V. E. M., and Buxton, R. B. (2011). A theoretical framework for estimating cerebral oxygen metabolism changes using the calibrated-BOLD method: modeling the effects of blood volume distribution, hematocrit, oxygen extraction fraction, and tissue signal properties on the BOLD signal. *Neuroimage* 58, 198–212. doi: 10.1016/j.neuroimage.2011.05.077
- Halani, S., Kwinta, J. B., Golestani, A. M., Khatamian, Y. B., and Chen, J. J. (2015). Comparing cerebrovascular reactivity measured using BOLD and cerebral blood flow MRI: the effect of basal vascular tension on vasodilatory and vasoconstrictive reactivity. *Neuroimage* 110, 110–123. doi: 10.1016/j.neuroimage.2015.01.050
- Hardie, J. A., Vollmer, W. M., Buist, A. S., Ellingsen, I., and Mørkve, O. (2004). Reference values for arterial blood gases in the elderly. *Chest* 125, 2053–2060. doi: 10.1378/chest.125.6.2053
- Hoge, R. D. (2012). Calibrated fMRI. *Neuroimage* 62, 930–937. doi: 10.1016/j.neuroimage.2012.02.022
- Hoge, R. D., Atkinson, J., Gill, B., Crelier, G. R., Marrett, S., and Pike, G. B. (1999a). Investigation of BOLD signal dependence on cerebral blood flow and oxygen consumption: the deoxyhemoglobin dilution model. *Magn. Reson. Med.* 42, 849–863. doi: 10.1002/(sici)1522-2594(199911)42:5<849::aid-mrm4>3.0.co;2-z
- Hoge, R. D., Atkinson, J., Gill, B., Crelier, G. R., Marrett, S., and Pike, G. B. (1999b). Linear coupling between cerebral blood flow and oxygen consumption in activated human cortex. *Proc. Natl. Acad. Sci. U. S. A.* 96, 9403–9408. doi: 10.1073/pnas.96.16.9403
- Hülsman, W. C., and Dubelaar, M. L. (1988). Aspects of fatty acid metabolism in vascular endothelial cells. *Biochimie* 70, 681–686. doi: 10.1016/0300-9084(88)90253-2
- Iadecola, C. (2017). The neurovascular unit coming of age: a journey through neurovascular coupling in health and disease. *Neuron* 96, 17–42. doi: 10.1016/j.neuron.2017.07.030
- Iadecola, C., Arneric, S. P., Baker, H. D., Tucker, L. W., and Reis, D. J. (1987). Role of local neurons in cerebrocortical vasodilation elicited from cerebellum. *Am. J. Physiol.* 252, R1082–R1091.
- Iadecola, C., and Zhang, F. (1994). Nitric oxide-dependent and -independent components of cerebrovasodilation elicited by hypercapnia. *Am. J. Physiol.* 266, R546–R552.
- Iadecola, C., and Zhang, F. (1996). Permissive and obligatory roles of NO in cerebrovascular responses to hypercapnia and acetylcholine. *Am. J. Physiol.* 271, R990–R1001.
- Iadecola, C., Zhang, F., and Xu, X. (1993). Role of nitric oxide synthase-containing vascular nerves in cerebrovasodilation elicited from cerebellum. *Am. J. Physiol.* 264, R738–R746.
- Jahanian, H., Christen, T., Moseley, M. E., Pajewski, N. M., Wright, C. B., Tamura, M. K., et al. (2017). Measuring vascular reactivity with resting-state blood oxygenation level-dependent (BOLD) signal fluctuations: a potential alternative to the breath-holding challenge? *J. Cerebral Blood Flow Metab.* 37, 2526–2538. doi: 10.1177/0271678x16670921
- Jain, V., Langham, M. C., Floyd, T. F., Jain, G., Magland, J. F., and Wehrli, F. W. (2011). Rapid magnetic resonance measurement of global cerebral metabolic rate of oxygen consumption in humans during rest and hypercapnia. *J. Cerebr. Blood Flow Metab.* 31, 1504–1512. doi: 10.1038/jcbfm.2011.34
- Jia, X.-Z., Sun, J.-W., Ji, G.-J., Liao, W., Lv, Y.-T., Wang, J., et al. (2020). Percent amplitude of fluctuation: a simple measure for resting-state fMRI signal at single voxel level. *PLoS One* 15:e0227021. doi: 10.1371/journal.pone.0227021
- Kannurpatti, S. S., Biswal, B. B., Kim, Y. R., and Rosen, B. R. (2008). Spatio-temporal characteristics of low-frequency BOLD signal fluctuations in isoflurane-anesthetized rat brain. *Neuroimage* 40, 1738–1747. doi: 10.1016/j.neuroimage.2007.05.061
- Kannurpatti, S. S., Motes, M. A., Biswal, B. B., and Rypma, B. (2014). Assessment of unconstrained cerebrovascular reactivity marker for large age-range fMRI studies. *PLoS One* 9:e88751. doi: 10.1371/journal.pone.0088751
- Kannurpatti, S. S., Motes, M. A., Rypma, B., and Biswal, B. B. (2010). Neural and vascular variability and the fMRI-BOLD response in normal aging. *Magn. Reson. Imaging* 28, 466–476. doi: 10.1016/j.mri.2009.12.007
- Kannurpatti, S. S., Motes, M. A., Rypma, B., and Biswal, B. B. (2011). BOLD signal change: minimizing vascular contributions by resting-state-fluctuation-of-amplitude scaling. *Hum. Brain Mapp.* 32, 1125–1140. doi: 10.1002/hbm.21097
- Komori, M., Takada, K., Tomizawa, Y., Nishiyama, K., Kawamata, M., and Ozaki, M. (2007). Permissive range of hypercapnia for improved peripheral microcirculation and cardiac output in rabbits. *Crit. Care Med.* 35, 2171–2175. doi: 10.1097/01.ccm.0000281445.77223.31
- Lajoie, I., Nugent, S., Debacker, C., Dyson, K., Tancredi, F. B., Badhwar, A., et al. (2017). Application of calibrated fMRI in Alzheimer's disease. *Neuroimage Clin.* 15, 348–358.
- Leopold, D. A., and Maier, A. (2012). Ongoing physiological processes in the cerebral cortex. *Neuroimage* 62, 2190–2200. doi: 10.1016/j.neuroimage.2011.10.059
- Lewis, N., Lu, H., Liu, P., Hou, X., Damaraju, E., Iraj, A., et al. (2020). Static and dynamic functional connectivity analysis of cerebrovascular reactivity: An fMRI study. *Brain Behav.* 10:e01516.
- Liu, P., Hebrank, A. C., Rodrigue, K. M., Kennedy, K. M., Section, J., Park, D. C., et al. (2013). Age-related differences in memory-encoding fMRI responses after accounting for decline in vascular reactivity. *Neuroimage* 78, 415–425. doi: 10.1016/j.neuroimage.2013.04.053
- Liu, P., Li, Y., Pinho, M., Park, D. C., Welch, B. G., and Lu, H. (2017). Cerebrovascular reactivity mapping without gas challenges. *Neuroimage* 146, 320–326. doi: 10.1016/j.neuroimage.2016.11.054
- Liu, T. T. (2013). Neurovascular factors in resting-state functional MRI. *NeuroImage* 80, 339–348. doi: 10.1016/j.neuroimage.2013.04.071
- Liu, Z., de Zwart, J. A., Chang, C., Duan, Q., van Gelderen, P., and Duyn, J. H. (2014). Neuroelectrical decomposition of spontaneous brain activity measured with functional magnetic resonance imaging. *Cerebr. Cortex* 24, 3080–3089. doi: 10.1093/cercor/bht164
- Liu, Z., Rios, C., Zhang, N., Yang, L., Chen, W., and He, B. (2010). Linear and nonlinear relationships between visual stimuli, EEG and BOLD fMRI signals. *Neuroimage* 50, 1054–1066. doi: 10.1016/j.neuroimage.2010.01.017
- Mark, C. I., Mazerolle, E. L., and Chen, J. J. (2015). Metabolic and vascular origins of the BOLD effect: Implications for imaging pathology and resting-state brain function. *J. Magn. Reson. Imaging* 42, 231–246. doi: 10.1002/jmri.24786
- Mazerolle, P., Philouze, P., Garrel, R., Aubry, K., Morinière, S., El Bedoui, S., et al. (2018). Oncological and functional outcomes of trans-oral robotic surgery for pyriform sinus carcinoma: a french GETTEC group study. *Oral Oncol.* 86, 165–170. doi: 10.1016/j.oraloncology.2018.09.014
- Mishra, A., Reynolds, J. P., Chen, Y., Gourine, A. V., Rusakov, D. A., and Attwell, D. (2016). Astrocytes mediate neurovascular signaling to capillary pericytes but not to arterioles. *Nat. Neurosci.* 19, 1619–1627. doi: 10.1038/nn.4428
- Najarian, T., Marrache, A. M., Dumont, I., Hardy, P., Beauchamp, M. H., Hou, X., et al. (2000). Prolonged hypercapnia-evoked cerebral hyperemia via K(+) channel- and prostaglandin E(2)-dependent endothelial nitric oxide synthase induction. *Circ. Res.* 87, 1149–1156. doi: 10.1161/01.res.87.12.1149

- Olafsson, V., Kundu, P., Wong, E. C., Bandettini, P. A., and Liu, T. T. (2015). Enhanced identification of BOLD-like components with multi-echo simultaneous multi-slice (MESMS) fMRI and multi-echo ICA. *Neuroimage* 112, 43–51. doi: 10.1016/j.neuroimage.2015.02.052
- Peebles, K. C., Richards, A. M., Celi, L., McGrattan, K., Murrell, C. J., and Ainslie, P. N. (2008). Human cerebral arteriovenous vasoactive exchange during alterations in arterial blood gases. *J. Appl. Physiol.* 105, 1060–1068. doi: 10.1152/jappphysiol.90613.2008
- Pelligrino, D. A., Santizo, R. A., and Wang, Q. (1999). Miconazole represses CO<sub>2</sub>-induced pial arteriolar dilation only under selected circumstances. *Am. J. Physiol.* 277, H1484–H1490.
- Pinto, J., Bright, M. G., Bulte, D. P., and Figueiredo, P. (2020). Cerebrovascular reactivity mapping without gas challenges: a methodological guide. *Front. Physiol.* 11:608475. doi: 10.3389/fphys.2020.608475
- Poublanc, J., Crawley, A. P., Sobczyk, O., Montandon, G., Sam, K., Mandell, D. M., et al. (2015). Measuring cerebrovascular reactivity: the dynamic response to a step hypercapnic stimulus. *J. Cereb. Blood Flow Metab.* 35, 1746–1756. doi: 10.1038/jcbfm.2015.114
- Preibisch, C., Castrillón, G. J. G., Bührer, M., and Riedl, V. (2015). Evaluation of multiband EPI acquisitions for resting state fMRI. *PLoS One* 10:e0136961. doi: 10.1371/journal.pone.0136961
- Rack-Gomer, A. L., and Liu, T. T. (2012). Caffeine increases the temporal variability of resting-state BOLD connectivity in the motor cortex. *Neuroimage* 59, 2994–3002. doi: 10.1016/j.neuroimage.2011.10.001
- Rancillac, A., Rossier, J., Guille, M., Tong, X.-K., Geoffroy, H., Amatore, C., et al. (2006). Glutamatergic control of microvascular tone by distinct GABA neurons in the cerebellum. *J. Neurosci.* 26, 6997–7006. doi: 10.1523/jneurosci.5515-05.2006
- Sanganahalli, B. G., Herman, P., Rothman, D. L., Blumenfeld, H., and Hyder, F. (2016). Metabolic demands of neural-hemodynamic associated and disassociated areas in brain. *J. Cereb. Blood Flow Metab.* 36, 1695–1707. doi: 10.1177/0271678x16664531
- Shmuel, A., Augath, M., Oeltermann, A., and Logothetis, N. K. (2006). Negative functional MRI response correlates with decreases in neuronal activity in monkey visual area V1. *Nat. Neurosci.* 9, 569–577. doi: 10.1038/nn1675
- Shmueli, K., van Gelderen, P., de Zwart, J. A., Horowitz, S. G., Fukunaga, M., Jansma, J. M., et al. (2007). Low-frequency fluctuations in the cardiac rate as a source of variance in the resting-state fMRI BOLD signal. *Neuroimage* 38, 306–320. doi: 10.1016/j.neuroimage.2007.07.037
- Shokri-Kojori, E., Tomasi, D., and Volkow, N. D. (2018). An autonomic network: synchrony between slow rhythms of pulse and brain resting state is associated with personality and emotions. *Cerebral Cortex* 28, 3356–3371. doi: 10.1093/cercor/bhy144
- Slowik, J. M., and Collen, J. F. (2020). *Obstructive Sleep Apnea*. Treasure Island, FL: StatPearls Publishing.
- Specht, K. (2019). Current challenges in translational and clinical fMRI and future directions. *Front. Psychiatry* 10:924. doi: 10.3389/fpsy.2019.00924
- Stefanovic, B., Schwindt, W., Hoehn, M., and Silva, A. C. (2007). Functional uncoupling of hemodynamic from neuronal response by inhibition of neuronal nitric oxide synthase. *J. Cereb. Blood Flow Metab.* 27, 741–754. doi: 10.1038/sj.jcbfm.9600377
- Stefanovic, B., Warnking, J. M., Rylander, K. M., and Pike, G. B. (2006). The effect of global cerebral vasodilation on focal activation hemodynamics. *Neuroimage* 30, 726–734. doi: 10.1016/j.neuroimage.2005.10.038
- Tak, S., Polimeni, J. R., Wang, D. J. J., Yan, L., and Chen, J. J. (2015). Associations of resting-state fMRI functional connectivity with flow-BOLD coupling and regional vasculature. *Brain Connect.* 5, 137–146. doi: 10.1089/brain.2014.0299
- Tancredi, F. B., Gauthier, C. J., Madjar, C., Bolar, D. S., Fisher, J. A., Wang, D. J. J., et al. (2012). Comparison of pulsed and pseudocontinuous arterial spin-labeling for measuring CO<sub>2</sub>-induced cerebrovascular reactivity. *J. Magn. Reson. Imaging* 36, 312–321. doi: 10.1002/jmri.23658
- Taneja, K., Lu, H., Welch, B. G., Thomas, B. P., Pinho, M., Lin, D., et al. (2019). Evaluation of cerebrovascular reserve in patients with cerebrovascular diseases using resting-state MRI: a feasibility study. *Magn. Reson. Imaging* 59, 46–52. doi: 10.1016/j.mri.2019.03.003
- Thompson, G. J., Riedl, V., Grimmer, T., Drzezga, A., Herman, P., and Hyder, F. (2016). The whole-brain “Global” signal from resting state fMRI as a potential biomarker of quantitative state changes in glucose metabolism. *Brain Connect.* 6, 435–447. doi: 10.1089/brain.2015.0394
- Todd, N., Josephs, O., Zeidman, P., Flandin, G., Moeller, S., and Weiskopf, N. (2017). Functional sensitivity of 2D simultaneous multi-slice echo-planar imaging: effects of acceleration on g-factor and physiological noise. *Front. Neurosci.* 11:158. doi: 10.3389/fnins.2017.00158
- Tong, Y., and Frederick, B. D. (2010). Time lag dependent multimodal processing of concurrent fMRI and near-infrared spectroscopy (NIRS) data suggests a global circulatory origin for low-frequency oscillation signals in human brain. *Neuroimage* 53, 553–564. doi: 10.1016/j.neuroimage.2010.06.049
- Tong, Y., and Frederick, B. D. (2014). Tracking cerebral blood flow in BOLD fMRI using recursively generated regressors. *Hum. Brain Mapp.* 35, 5471–5485. doi: 10.1002/hbm.22564
- Triantafyllou, C., Hoge, R. D., Krueger, G., Wiggins, C. J., Potthast, A., Wiggins, G. C., et al. (2005). Comparison of physiological noise at 1.5 T, 3 T and 7 T and optimization of fMRI acquisition parameters. *Neuroimage* 26, 243–250. doi: 10.1016/j.neuroimage.2005.01.007
- Tsvetanov, K. A., Henson, R. N. A., Jones, P. S., Mutsaerts, H., Fuhrmann, D., Tyler, L. K., et al. (2020). The effects of age on resting-state BOLD signal variability is explained by cardiovascular and cerebrovascular factors. *Psychophysiology* 2020:e13714.
- Tsvetanov, K. A., Henson, R. N. A., Tyler, L. K., Davis, S. W., Shafto, M. A., Taylor, J. R., et al. (2015). The effect of ageing on fMRI: Correction for the confounding effects of vascular reactivity evaluated by joint fMRI and MEG in 335 adults. *Hum. Brain Mapp.* 36, 2248–2269. doi: 10.1002/hbm.22768
- Uladak, K., Dubowitz, D. J., Yoder, E. J., Restom, K., Liu, T. T., and Buxton, R. B. (2004). Coupling of cerebral blood flow and oxygen consumption during physiological activation and deactivation measured with fMRI. *Neuroimage* 23, 148–155. doi: 10.1016/j.neuroimage.2004.05.013
- Van Dijk, K. R. A., Hedden, T., Venkataraman, A., Evans, K. C., Lazar, S. W., and Buckner, R. L. (2010). Intrinsic functional connectivity as a tool for human connectomics: theory, properties, and optimization. *J. Neurophysiol.* 103, 297–321. doi: 10.1152/jn.00783.2009
- Vogt, K. M., Ibrinson, J. W., Schmalbrock, P., and Small, R. H. (2011). Comparison between end-tidal CO<sub>2</sub> and respiration volume per time for detecting BOLD signal fluctuations during paced hyperventilation. *Magn. Reson. Imaging* 29, 1186–1194. doi: 10.1016/j.mri.2011.07.011
- Wang, Q., Pelligrino, D. A., Koenig, H. M., and Albrecht, R. F. (1994). The role of endothelium and nitric oxide in rat pial arteriolar dilatory responses to CO<sub>2</sub> in vivo. *J. Cereb. Blood Flow Metab.* 14, 944–951. doi: 10.1038/jcbfm.1994.126
- Wise, R. G., Harris, A. D., Stone, A. J., and Murphy, K. (2013). Measurement of OEF and absolute CMRO<sub>2</sub>: MRI-based methods using interleaved and combined hypercapnia and hyperoxia. *Neuroimage* 83, 135–147. doi: 10.1016/j.neuroimage.2013.06.008
- Xu, F., Uh, J., Brier, M. R., Hart, J., Yezhuvath, U. S., Gu, H., et al. (2011). The influence of carbon dioxide on brain activity and metabolism in conscious humans. *J. Cerebral Blood Flow Metab.* 31, 58–67. doi: 10.1038/jcbfm.2010.153
- Yao, J. F., Yang, H.-C. S., Wang, J. H., Liang, Z., Talavage, T. M., Tamer, G. G. Jr., et al. (2021). A novel method of quantifying hemodynamic delays to improve hemodynamic response, and CVR estimates in CO<sub>2</sub> challenge fMRI. *J. Cereb. Blood Flow Metab.* 2021:271678X20978582.
- Zou, Q. H., Zhu, C. Z., Yang, Y., Zuo, X. N., Long, X. Y., Cao, Q. J., et al. (2008). An improved approach to detection of amplitude of low-frequency fluctuation (ALFF) for resting-state fMRI: fractional ALFF. *J. Neurosci. Methods* 172, 137–141. doi: 10.1016/j.jneumeth.2008.04.012

**Conflict of Interest:** The authors declare that the research was conducted in the absence of any commercial or financial relationships that could be construed as a potential conflict of interest.

Copyright © 2021 Chen and Gauthier. This is an open-access article distributed under the terms of the Creative Commons Attribution License (CC BY). The use, distribution or reproduction in other forums is permitted, provided the original author(s) and the copyright owner(s) are credited and that the original publication in this journal is cited, in accordance with accepted academic practice. No use, distribution or reproduction is permitted which does not comply with these terms.